

Molecularly imprinted polymer prepared by Pickering emulsion polymerization for removal of acephate residues from contaminated waters

Xiaoping Luo,¹ Changzheng Li,¹ Yuqing Duan,¹ Haihui Zhang,¹ Di Zhang,¹ Can Zhang,¹ Guibo Sun,² Xiaobo Sun^{2,3}

¹School of Food and Biological Engineering, Jiangsu University, Zhenjiang 212013, China

²Institute of Medicinal Plants, Chinese Academy of Medical Sciences, Beijing 100193, China

³School of Chemistry & Chemical Engineering, Jiangsu University, Zhenjiang 212013, China

Correspondence to: Y. Duan (E-mail: dyq101@mail.ujs.edu.cn) and X. Sun (E-mail: xbsun@imiplad.ac.cn)

ABSTRACT: A molecularly imprinted polymer (MIP) prepared with Pickering emulsion polymerization was designed by a computational approach for removal of acephate from aqueous solution. Methacrylic acid, ethylene glycol dimethacrylate, and chloroform were screened as the optimal functional monomer, crosslinker, and porogen by the Gaussian 03 package using the density functional theory method. The polymerization was carried out in an oil-in-water emulsion using nano-SiO₂ particles as stabilizer instead of a toxic surfactant. The characterization results indicated that the prepared MIP had a porous and hollow core, and the particle size was approximately 20 μm. The binding and recognition abilities of MIP for acephate were studied through equilibrium adsorption analysis and selectivity analysis. The results showed that the MIP had high binding capacity and excellent selectivity for acephate. The saturated binding amount could reach 6.59 × 10³ μg/g. The Langmuir isotherm model gave a good fit to the experimental data. Moreover, the results of a reusability analysis and practical application suggested that the prepared MIP provides the potential for removal of acephate residues from aqueous solution. © 2015 Wiley Periodicals, Inc. *J. Appl. Polym. Sci.* **2016**, , 43126.

KEYWORDS: adsorption; applications; emulsion polymerization; theory and modeling

Received 16 September 2015; accepted 2 November 2015

DOI: 10.1002/app.43126

INTRODUCTION

Organophosphorus pesticides (OPPs) are widely used as insecticides for insect pest control in farming because of their high effectiveness and low cost. Most of them are highly toxic to animals, including human beings, in which acetylcholinesterase takes a significant role.¹ Many OPPs can accumulate in organisms and cause serious diseases.² Acephate, a water-soluble OPP, is a good alternative to high-toxicity OPPs in agriculture on a global scale because of its broad spectrum and high efficiency, and its production is even increasing in some countries. With the generous use of acephate, people may be exposed to it mainly through residues in water and from other contaminated organisms. Moreover, acephate is known to degrade to an extremely hazardous OPP, methamidophos, by bacteria in the presence of oxygen.³ Due to the potential security and ecological risks, the removal of acephate residues is highly valuable.

Up to now, several methods have been used for degradation and removal of OPPs from water or other contaminated substrate. Organophosphorus hydrolases play a critical function in the degradation and purification of OPPs, such as isofenphos-methyl hydrolase⁴ and extracellular fungal organophosphate hydrolases,⁵ which were reported to hydrolyze OPPs under the optimized conditions. Over the past 20 years, numerous publications applied the photocatalysis method for degradation of OPPs in contaminated water. For example, TiO₂ nanoparticles,⁶ zinc oxide,⁷ and metal ions⁸ used as photocatalysts were reported. In addition, many new methods were also developed to remove OPPs in recent years, such as biodegradation,⁹ microwave degradation,¹⁰ phytoremediation,¹¹ biomineralization,¹² ultrasonic irradiation degradation,¹³ electrochemical degradation,¹⁴ zeolitic material sorption,¹⁵ activated carbon sorption,¹⁶ nanofiltration,¹⁷ and silver-nanobiohybride material sorption.¹⁸ Most of these methods are effective in decontamination of OPP residues in contaminated water, but the main

Additional Supporting Information may be found in the online version of the article.

© 2015 Wiley Periodicals, Inc.

disadvantages, such as being nonspecific, energy consuming, unstable, and time consuming, still exist. Accordingly, development of a selective adsorption method to remove acephate residues is still called for. In order to overcome these defects, a selective adsorption material, a molecularly imprinted polymer (MIP), used as adsorbent for the removal of OPP residues from a dichloromethane solution has been developed.¹⁹

MIP, a man-made polymeric macromolecule, is normally prepared in a suitable porogen containing functional monomers, crosslinker, and initiator in the presence of a template.²⁰ After removal of the template from the polymer, three-dimensional specific recognition sites were formed, which are complementary in size, shape, and spatial distribution to the template molecule.²¹ Recently, MIPs have attracted increasing attention because of their fine mechanical and chemical stability, recognition property, low cost, and simple preparation. MIPs have been utilized in many fields, including sample preparation,²² controlled drug delivery systems,²³ catalytic applications,²⁴ artificial antibodies,²⁵ separations,²⁶ removal of phenols from contaminated waters,²⁷ and sensor components.²⁸ In recent years, MIPs have been widely used to selectively recognize and remove target pollutants.²⁹

Typically, MIPs are prepared by bulk polymerization, dispersion polymerization, precipitation polymerization, suspension polymerization, and in situ polymerization.³⁰ Recently, Pickering emulsion polymerization has attracted attention and has been introduced for the preparation of MIPs by Ye.³¹ As we know, Pickering emulsions, in which dispersed liquid droplets are stabilized by small solid particles attached to the droplet surfaces,³² form either oil-in-water or water-in-oil systems.³³ Compared to conventional polymerizations, Pickering emulsion polymerization has advantages as follows: (1) it can generate highly water compatible MIP, making the MIP show specific recognition properties in water,³⁴ and (2) it can form a uniform polymer layer, which offers fast binding and releasing kinetics for the template molecules.

Traditionally, the optimization of a polymerization system (functional monomer, porogen, and crosslinker) is based on labor-intensive, time-consuming experimental trials. In order to reduce the experimental time and the use of hazardous reagents, the computational approach has been applied to the design of MIPs by calculating the binding energy between the template and the monomer or crosslinker.³⁵ Selections of monomer,^{36,37} porogen,³⁸ and crosslinker³⁹ by the computational approach have been reported over the last decade. In this work, we report the simultaneous optimization of monomer, porogen, and crosslinker for rational design of MIPs by a computational approach using the density functional theory (DFT) method. An MIP was then synthesized in bare nano-SiO₂ particles in a stabilized oil-in-water Pickering emulsion. In our polymerization system, we mixed monomer, ethylene glycol dimethacrylate (EGDMA), and azobisisobutyronitrile (AIBN) in chloroform as the oil phase and added nano-SiO₂ into water as the water phase. The characterization of the MIP was investigated and discussed. The adsorption kinetics, isotherm, and selectivity of the MIP toward acephate were studied. In addition, the reus-

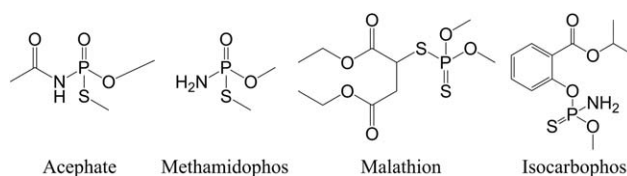


Figure 1. Molecular structures of acephate, methamidophos, malathion, and isocarbophos.

ability of the MIP was evaluated. Finally, the prepared MIP was also used for purification of practical water samples.

EXPERIMENTAL

Materials and Reagents

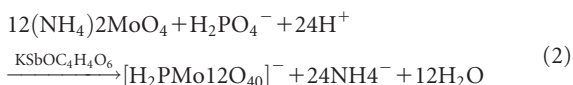
Acephate (99%) was bought from National Pesticide Quality Control Center (Shenyang, China) and used as a template. Methamidophos, malathion, and isocarbophos (99%) obtained from Shanghai Pesticide Research Institute (Shanghai, China) were used as analogs. The chemical structures of acephate and its analogs are shown in Figure 1. Methacrylic acid (MAA, 98%), ethylene glycol dimethacrylate (EGDMA, 98%), and azobisisobutyronitrile (AIBN, 98%) were purchased from Sigma-Aldrich (Gillingham, UK). AIBN was recrystallized from methanol. MAA and EGDMA were distilled under reduced pressure to remove their stabilizer prior to use. Nano-SiO₂ particles (diameter 20 nm), purchased from Hehai Nanometer Science & Technology Co., Ltd. (Taixing, China), were activated according to the reported method⁴⁰ before use. All other chemicals used in this study were of analytical grade and used without any further purification.

Instruments and Apparatus

Fourier transform infrared (FTIR) spectra (4000–400 cm⁻¹) were recorded on a Nicolet NEXUS-670 FTIR spectrometer (San Carlos, CA). The morphology of MIP was observed by scanning electron microscopy (SEM) with a Hitachi S-3400N (Tokyo, Japan). The optical micrographs of the Pickering emulsion and MIP were collected by a Leica DMI4000B optical microscope (Munich, Germany).

Detection of Acephate

In this work, the concentration of acephate was detected by a modified phospho-molybdenum blue method that was reported by Murphy,⁴¹ using a Cary-100 Varian spectrophotometer (Palo Alto, CA). For the digestion, the acephate solution (3 mL) and K₂S₂O₈ (2.5%, 7 mL) were added into a Teflon digestion tank and reacted at 140°C for 1 h, then cooled at room temperature. Then for the chromogenic reaction, after transferring the digestion liquid (2 mL) into a colorimetric tube (20 mL), ultrapure water (3.6 mL), H₂SO₄ (3.0 mol/L, 1.2 mL), ammonium molybdate (2.5%, 0.6 mL, containing 0.07% of antimony potassium), and ascorbic acid (0.6 mL) were added in succession with shaking for 10 s. Subsequently, the tube was placed in a thermostated water bath at 90°C for 45 min. Finally, for measurement, the colored solution was cooled for 30 min before the absorbance readings were taken at 710 nm. The principle of this method is shown as follows:



Computational Simulation

A computational approach was employed to investigate the interaction between template and functional monomer (or crosslinker). All computer simulations were carried out using the Gaussian 03 program package.⁴²

The conformations of template, monomers, crosslinker, template–monomer complexes, and template–(crosslinker) complexes were generated using the ChemBioOffice (Cambridge, Massachusetts) 2010 program and then optimized using the Hartree–Fock (HF) method at the 3-21G basis set⁴³ and density functional theory (DFT) method at the Becke, three-parameter, Lee–Yang–Parr (B3LYP) level with the 6-31G basis set⁴⁴ in vacuum. Subsequently, the electronic energies of the monomers, template, crosslinker, and complexes with the optimal conformations were also calculated through the same method. Finally, the binding energies (ΔE) of template–monomer complexes and template–(crosslinker) complexes in vacuum were calculated using the following equation⁴⁵:

$$\Delta E_{(\text{vacuum})} = E_{(\text{complex})} - E_{(\text{template})} - E_{(\text{monomer/crosslinker})} \quad (4)$$

where $E_{(\text{complex})}$ is the interaction energy of the complex of monomers/crosslinker and acephate in vacuum, and $E_{(\text{template})}$ and $E_{(\text{monomer/crosslinker})}$ are the energy levels of acephate and monomers/crosslinker in vacuum, respectively.

In this work, a larger virtual library of 21 kinds of frequently used functional monomers and nine kinds of crosslinkers was designed and screened against the molecular template. The HF method with 3-21G basis set was used to screen the functional monomer and crosslinker for their possible interactions with acephate, and the results for the binding energy of each monomer and crosslinker reacting with acephate are shown in Tables I and II. The screened monomers and crosslinkers were further optimized by using the DFT method at the B3LYP level with the 6-31G basis set in vacuum.

Furthermore, solvent effects were estimated using the polarizable continuum model (PCM) developed by Tomasi and coworkers.⁴⁶ Electronic energies in solvent were also calculated through the DFT method at the B3LYP level with the 6-31G basis set. The solvent effects of a complex in solvent were calculated from the equation

$$\Delta E_{(\text{solvent})} = \Delta E_{(\text{solvent})} - \Delta E_{(\text{vacuum})} \quad (5)$$

where $\Delta E_{(\text{solvent})}$ and $\Delta E_{(\text{vacuum})}$ are the binding energies of complexes in solvent and in vacuum, respectively.

Preparation of MIP Particles

The MIP was prepared according to the Pickering emulsion polymerization method reported by Ye.⁴⁷ First, the oil phase was prepared. Acephate (0.5 mmol) and MAA (1.5 mmol) were

dissolved in chloroform (0.5 mL). This mixture solution was ultrasonically dispersed for 5.0 min and then kept standing for 4 h to obtain the prepolymerization solution. EGDMA (7.5 mmol) and AIBN (20 mg) were added into the prepolymerization solution and dissolved with shaking. Second, the water phase was obtained. Nano-SiO₂ particles (0.2 g) were added into ultrapure water (6 mL) and sonicated for 5 min. Third, the Pickering emulsion was established. The oil phase was added into the water phase and the pH adjusted to 5.5 with a NaOH solution (3.0 mol/L). Then, the mixture was again sonicated for 5 min to form the Pickering emulsion. Finally, the MIP was prepared. After purging oxygen with nitrogen gas for 5 min, the temperature was increased to 70°C and kept for 16 h without agitation. Following this polymerization procedure, the obtained particles were washed with water and ethanol and then stirred in HF (30%, 5 mL) at room temperature for 12 h to remove the nano-SiO₂ particles. After this step, the polymers were washed with methanol/acetic acid (90/10, v/v) by Soxhlet apparatus for 48 h. Finally, the MIP particles were obtained by filtration, washing, and drying. As a control, the nonimprinted polymer (NIP) was also prepared in the same way but without adding the template.

Adsorption Experiments

The binding kinetics was tested to evaluate the adsorption rate of the MIP or NIP for the template molecules. MIP or NIP (20 mg) was added to an acephate solution (100 μg/mL, 5 mL) and incubated for different times (15, 30, 45, 60, 90, 120, 180, 240, 300, 360, 420, and 480 min).

Meanwhile, the static binding capacity of MIP or NIP was measured by suspending MIP and NIP (20 mg) in ultrapure water (5 mL) with different acephate concentrations (5–100 μg/mL). The mixtures were vortically incubated at room temperature for 3 h, and the supernatant solution was separated through a 0.22 μm microporous membrane. The binding amount of acephate on MIP was determined by measuring the difference between total acephate amount and residual amount in solution by the phospho-molybdenum blue method.

The selective recognition ability of MIP was investigated using the structure analogs methamidophos, malathion, and isocarbo-phos as interferents with acephate. MIP or NIP (20 mg) was added into acephate (0.5 μmol/mL, 5 mL) or analogs at the same molarity with acephate.

The binding capacity (Q) was defined as the total amount of acephate adsorbed per gram of the MIP. The binding capacities (μg/g) of MIP were calculated from the equation

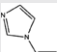

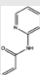
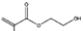


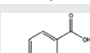
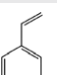
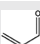


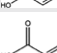
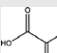
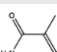
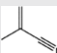
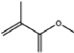
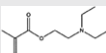
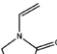
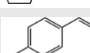
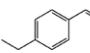
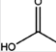
$$Q = \frac{(C_0 - C_t)V1000}{Mm} \quad (6)$$

where C_0 and C_t are the initial and residual concentrations (μg/mL) of acephate or the analog, respectively, M (g/mol) is the molar mass of the template (or analog), m (mg) is the weight of MIP or NIP used for the adsorption experiments, and V (mL) is the volume of the solution.

Reusability of MIP

MIP (20 mg) was added into ultrapure water (5 mL) with an acephate concentration of 100 μg/mL. After adsorption and

Table I. Library of Monomers and Binding Energies for Corresponding Template–Monomer Complexes by HF Method at B3LYP Level with 3-21G Basis Set in Vacuum

Monomer	Structural formula	ΔE (hartree) ^a	ΔE (KJ/mol)
1-Vinylimidazole		-0.0184643	-11.58653289
2-Acrylamide-2-methyl-propane sulfonic acid		-0.0139922	-8.780245422
2-Acrylamidopyridine		-0.0128064	-8.036144064
2-Hydroxyethyl methacrylate		-0.0159286	-9.995355786
2-Vinylpyridine		-0.0168027	-10.54386228
3-(Methacryloxy)propyltrimethoxysilane		-0.0128914	-8.089482414
4-Vinylbenzoic acid		-0.0188511	-11.82925376
4-Vinylpyridine		-0.0112299	-7.046874549
Acrolein		-0.0313322	-19.66126882
Acrylamide		-0.0252789	-15.86276254
Acrylonitrile		-0.0283289	-17.77666804
Itaconic acid		-0.0191474	-12.01518497
Methacrylic acid		-0.0532128	-33.39156413
Methacrylamide		-0.0226814	-14.23280531
Methacrylonitrile		-0.0150516	-9.445029516
Methyl methacrylate		-0.0095964	-6.021836964
<i>N,N</i> -Diethylaminoethyl methacrylate		-0.0065995	-4.141252245
<i>N</i> -Vinyl-2-pyrrolidone		-0.0142463	-8.939695713
<i>P</i> -Aminostyrene		-0.0047603	-2.987135853
<i>P</i> -Ethylstyrene		-0.0201014	-12.61382951
Acrylic acid		-0.0514305	-32.27315306

^a 1 hartree = 2625.5 KJ/mol.

filtration, the adsorbed MIP was washed with methanol/acetic acid (90/10, v/v) and dried to constant weight. Then the MIP was reused for the adsorption of acephate.

Application to Environmental Water

Environmental water samples were collected from Jianshan Lake, Wenlong Reservoir, and Yangtze River (Zhenjiang, China) and tap water from the laboratory. Water samples were filtered through a 0.22 μm microfiltration membrane before use. MIP or NIP (20 mg)

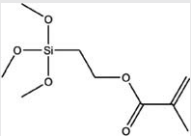
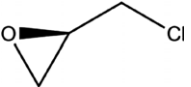
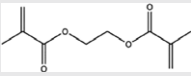

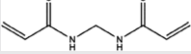
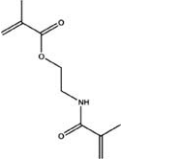
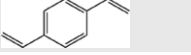
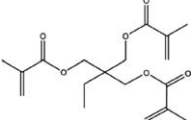
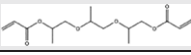
was added into a spiked water sample (5.0 mL, 10 $\mu\text{g}/\text{mL}$). After being shaken for 2 h at room temperature, the samples were filtered by a 0.22 μm microfiltration membrane, and the concentration of acephate was detected by the phospho-molybdenum blue method.

RESULTS AND DISCUSSION

Calibration Curve of Phospho-molybdenum Blue Method

The calibration curve is necessary to plot a relationship between the absorbance and the phosphate molar concentration in a UV

Table II. Library of Crosslinkers and Binding Energies for Corresponding Template–(Crosslinker) Complexes by HF Method at B3LYP Level with 3-21G Basis Set in Vacuum

Crosslinker	Structural formula	ΔE (hartree) ^a	ΔE (KJ/mol)
3-Methacryloxypropyltrimethoxysilane		-0.0128914	-8.089482414
Epichlorohydrin		-0.0143339	-8.994665589
EGDMA		-0.0111344	-6.986947344
Glutaraldehyde		-0.0237963	-14.93241621
N,N'-Methylene double acrylamide		-0.0283423	-17.78507667
N,O'-Bismethacryloyl ethanolamine		-0.02205244	-13.83812662
Divinylbenzene		-0.0190625	-11.96190938
Trimethylolpropane-3-methyl acrylate		-0.0159899	-10.03382215
TPGDA		-0.01753893	-11.00585396

^a1 hartree = 2625.5 KJ/mol.

spectrophotometry analysis. A standard phosphate solution (1.0 $\mu\text{mol/mL}$) was prepared by dissolving KH_2PO_4 (0.1361 g) in ultrapure water and diluted to 1000 mL.

From the standard solution, a series of KH_2PO_4 solutions were prepared. Then, the absorbance of the KH_2PO_4 solution was measured by UV spectrophotometry at 710 nm after the chromogenic reaction. The standard curve was constructed by plotting absorbance against molar concentration of phosphate (Figure 2). The linear regression equation of the calibration curve was $Y = 1.3187c + 0.0096$, with a correlation coefficient (R^2) of 0.9982. In addition, the limit of detection ($3\sigma/S$, IUPAC criteria)⁴⁸ was calculated to be $1.82 \times 10^{-3} \mu\text{mol/mL}$.

Computational Simulation

The selection of suitable monomer, crosslinker, and porogen is a crucial procedure in the polymerization process of MIP. In this work, a computational approach was applied to optimize the polymerization system.

Selection of Optimal Functional Monomer. From Table I, the preliminary work screened five kinds of monomers: acrolein (-19.66 KJ/mol), acrylonitrile (-17.78 KJ/mol), acrylamide (-15.86 KJ/mol), acrylic acid (-32.27 KJ/mol), and MAA (-33.39

KJ/mol). The further selection of monomer was applied by using the DFT method at the B3LYP level with the 6-31G basis set. Table III shows that the ΔE values with a given template are in the following order: $\Delta E_{(\text{MAA-acephate})} > \Delta E_{(\text{acrylic acid-acephate})} > \Delta E_{(\text{acrolein-acephate})} > \Delta E_{(\text{acrylamide-acephate})} > \Delta E_{(\text{acrylonitrile-acephate})} > \Delta E_{(\text{acrylamide-acephate})}$. According to the principle of choosing a monomer,⁴⁹ the MAA with the highest ΔE is more likely to form strong complexes with the template molecule. The optimal conformations of acephate and MAA are shown in Figure S1.

Selection of Optimal Crosslinker. From Table II, the initial work screened three kinds of crosslinker: EGDMA (-6.98 KJ/mol), epichlorohydrin (-8.99 KJ/mol), and tripropylene glycol diacrylate (TPGDA, -11.01 KJ/mol), respectively. The further calculated ΔE data (Table IV) of the interaction between crosslinker and template show that $\Delta E_{(\text{EGDMA-acephate})} < \Delta E_{(\text{epichlorohydrin-acephate})} < \Delta E_{(\text{TPGDA-acephate})}$, indicating that EGDMA gives the weakest binding energy with the template. According to previous research,³⁹ it is possible to suggest that EGDMA would be chosen as the optimal crosslinker for the polymerization of MIP because it would not affect the interaction between MAA and acephate. The optimal conformation of EGDMA is also displayed in Figure S1.

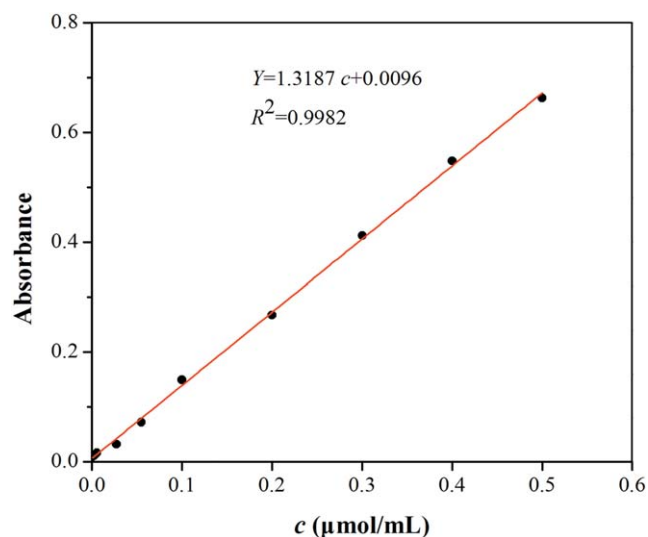


Figure 2. Calibration curve of phospho-molybdenum blue method (absorbance versus molar concentration of phosphate). [Color figure can be viewed in the online issue, which is available at wileyonlinelibrary.com.]

Selection of Optimal Porogen. The selectivity of MIP is usually affected by the porogen.⁵⁰ With acephate as template and MAA as monomer, the $\Delta E_{(\text{solv})}$ of eight kinds of solvents with different dielectric constants (ϵ) were also investigated by computational simulation. As observed (Table V), the results indicate that there is a good correlation between the $\Delta E_{(\text{solv})}$ and the ϵ of solvents. The higher the ϵ of the solvent, the higher is the $\Delta E_{(\text{solv})}$ of acephate or MAA in the solvent. It is obvious that we should choose chloroform, which can dissolve acephate and MAA with the lowest $\Delta E_{(\text{solv})}$, as the porogen for the preparation of the MIP since the solvent with low $\Delta E_{(\text{solv})}$ interfered with the interaction between template molecule and monomer to a small degree.

Spectrometric Analysis

The strength and location of the monomer–template interactions are significant to obtaining an MIP with good recognition properties. In order to investigate the interaction mechanism between monomer and template in the prepolymerized solution, the UV spectroscopic method⁵¹ was employed to study the recognition mechanism on a molecular level.

A series of solutions were prepared, each with a constant concentration of acephate (0.5 $\mu\text{mol/mL}$) and an increasing amount

of MAA (0–5 $\mu\text{mol/mL}$) in chloroform. The absorption spectra of those solutions with corresponding MAA solution as blank were determined. This interaction can be evaluated by the equation

$$\Delta A/b_0^n = -K\Delta A + K\Delta\epsilon a_0 l \quad (7)$$

where ΔA is the absorbance difference in chloroform solution before and after the reaction of acephate and MAA, b_0 is the concentration of MAA, n is the complex composition ($n = 1, 2, 3, \dots$), K is the association constant, ϵ is the absorbance coefficient, l is the inner diameter of the sample tank, and a_0 is the concentration of template. If a $\Delta A/b_0^n$ versus ΔA plot has a good linear relationship, the value of n is the optimal molar ratio of monomers and template in a prepolymerization solution.

In the present work, a linear plot can be observed at $n = 3$ in the curves of $\Delta A/b_0^n$ versus ΔA (Figure 3), which indicates that 1:3 MAA–acephate complexes are formed in the prepolymerization solution and have considerable stability. According to the slope of the linear curve at $n = 3$, the value of K is calculated to be $1.694 \times 10^4 \text{ L}^3/\text{mol}^3$ for the MAA–acephate complex compound.

Morphology of the Pickering Emulsion and MIP Surface

Photographs of the Pickering emulsion before (a) and after (b) ultrasonication are shown in Figure 4. The oil phase was located at the top of the vial, while the water phase dispersion with nano-SiO₂ particles was located at the bottom before ultrasonication. Then, a stable oil-in-water Pickering emulsion was obtained after ultrasonication. The optical micrographs of Pickering emulsions before (c) and after (d) polymerization clearly show that the oil droplets with a diameter of about 20 μm (in Pickering emulsions) were surrounded by some nano-SiO₂ particles, and no coacervation of the oil droplets could be observed. After polymerization, monodisperse microparticles were obtained. SEM was also used to assess the size and surface morphology of the pretreated MIP. The SEM micrograph (e) shows obviously a spherical shape approximately 20 μm in diameter for the prepared MIP, which was in agreement with the result in Figure 4(c). The surface morphology of MIP (f) became rough after removal of nano-SiO₂ particles. Moreover, a hollow core structure (g) and microporous surface (f) were also created on the MIP, which could benefit the binding site accessibility toward the template molecules.

Table III. Binding Energies for Template–Monomer Complexes by DFT Method at B3LYP Level with 6-31G Basis Set in Vacuum

Molecules	$E_{\text{acephate}/\text{monomer}}$	$E_{\text{monomer-template}}$	ΔE (hartree) ^a	ΔE (KJ/mol)
Acephate	-1178.2139559			
Acrolein	-191.8572558	-1370.094186	-0.0229743	-14.417
Acrylamide	-247.2251794	-1425.4550920	-0.01595671	-10.012
Acrylonitrile	-170.7839832	-1349.0185145	-0.0205754	-12.911
MAA	-306.3855834	-1484.6414546	-0.0419153	-26.302
Acrylic acid	-267.0770515	-1445.331234	-0.0402265	-25.243

^a1 hartree = 2625.5 KJ/mol.

Table IV. Binding Energies for Template–(Crosslinker) Complexes by DFT Method at B3LYP Level with 6-31G Basis Set in Vacuum

Molecules	$E_{\text{crosslinkers}}$	$E_{\text{crosslinkers-template}}$	ΔE (hartree) ^a	ΔE (KJ/mol)
Acephate	-1178.2139559			
EGDMA	-690.165275	-1868.3852903	-0.0060594	-3.80233
epichlorohydrin	-652.6182085	-1830.8410288	-0.0088644	-5.5625
TPGDA	-1037.0437405	-2215.2675589	-0.0098625	-6.18882

^a1 hartree = 2625.5 KJ/mol

FTIR Analysis

Figure 5 shows the FTIR spectra of NIP (a), MIP without (b) and after (c) extraction of the template molecule, and template (d). The characteristic peaks at 1731 cm^{-1} , 1261 cm^{-1} , and 1156 cm^{-1} obtained by NIP (curve a), which are attributed to the C=O stretching vibration of carboxyl from MAA and the C—O symmetric and asymmetric stretching vibrations of ester from EGDMA, also appeared in the spectra of MIP after extraction of the template (curve c). Meanwhile, the absorption peak at 3445 cm^{-1} of the polymer could be assigned to the stretching vibration of O—H bonds from the MAA molecule. All of these results confirm that the thermal polymerization was successful. For the template molecule (curve d), the features observed around 1245 cm^{-1} and 1224 cm^{-1} indicate the presence of a P=O bond; the broad peak at 1047 cm^{-1} represents the absorption of P—O—C. As promised, the absorption peak around 1230 cm^{-1} observed in the IR spectra (curve b) suggested the existence of a P=O bond on MIP without extraction of the template. Furthermore, compared with curve (d), the stretching shift of the P=O bond (curve b) could be attributed to the noncovalent interaction between the P=O group of the template and the —OH group of MAA. The FTIR analysis illustrates that acephate-imprinted MIP was successfully synthesized by Pickering emulsion polymerization.

Adsorption Studies

Some adsorption studies, such as adsorption kinetics, adsorption isotherms, Scatchard analysis, and selectivity analysis, were performed to evaluate the properties of the prepared MIP.

Adsorption Kinetics. Adsorption kinetics is crucial in evaluating the performance and adsorption mechanisms. The adsorp-

tion kinetics of acephate on MIP and NIP were studied in acephate solution ($100\text{ }\mu\text{g/mL}$) at different times. The kinetic binding curves (Figure 6) show that the amount of acephate adsorbed on MIP increased rapidly in the adsorption initial stage, and the adsorption equilibrium was achieved after adsorption for 3 h. Meanwhile, it could be clearly observed that MIP exhibits a much higher binding capacity and faster mass transfer than NIP, which could be attributed to the formation of rebinding sites for acephate in the MIP.

Adsorption Isotherms and Scatchard Analysis. The adsorption isotherm, critical to evaluating the binding capacity of MIP, is considered for understanding the interactions between acephate and MIP. In this work, two commonly used adsorption models, the Langmuir and Freundlich equations,⁵² were used to fit the experimental data, which can be expressed respectively as follows:

$$\frac{C_e}{Q_e} = \frac{C_e}{Q_m} + \frac{1}{KQ_m} \quad (8)$$

$$\log Q_e = \log K_f + \frac{1}{n} \log C_e \quad (9)$$

where Q_e is the equilibrium binding capacity ($\mu\text{g/g}$), C_e represents the equilibrium concentration ($\mu\text{g/mL}$) of acephate, Q_m is the maximum sorption capacity ($\mu\text{g/g}$), K is the adsorption equilibrium constant ($\text{mL}/\mu\text{g}$, related to the affinity of adsorption sites), K_f is a constant representing the binding capacity ($\mu\text{g/g}$), and n is an adsorption intensity.

The correlation coefficient (R^2) was applied to evaluate the applicability of the isotherm models to the adsorption behavior of MIP. Table VI shows that the adsorption behavior of the MIP was well fitted to the Langmuir isotherm model with higher

Table V. Electric Permittivity of Seven Solvents and Solvent Energies for Template–Monomer Complexes by DFT Method at B3LYP Level with 6-31G Basis Set in Corresponding Solvents

Solvent	ϵ	ΔE_1 (KJ/mol)	ΔE_2 (KJ/mol)	$\Delta E_{\text{solvent energy}}$ (KJ/mol) ^a
Acetonitrile	37.5	-26.302	-19.718	-6.58427
Methanol	33.6	-26.302	-19.7374	-6.56482
Water	80.4	-26.302	-19.6057	-6.6966
Chloroform	4.81	-26.302	-21.0524	-5.24987
Tetrahydrofuran	7.58	-26.302	-20.4954	-5.80691
Ethanol	24.3	-26.302	-19.8078	-6.49448
Dichloromethane	9.1	-26.302	-20.3312	-5.97107

^a1 hartree = 2625.5 KJ/mol.

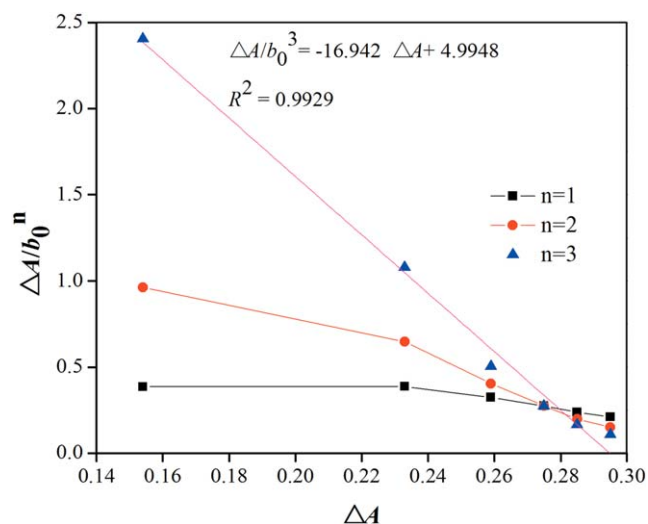


Figure 3. Curves of $\Delta A/b_0^n$ versus ΔA ; b_0 : concentration of MAA; ΔA : absorbance difference in chloroform solution before and after the reaction of the acephate molecule and MAA; n is the complex composition ($n = 1, 2, 3$). [Color figure can be viewed in the online issue, which is available at wileyonlinelibrary.com.]

values of R^2 , which could also be clearly seen in Figure S2. Moreover, the K_f for acephate on MIP is higher than it is on NIP, indicating the stronger recognition property of MIP for the template molecule.

The adsorption isotherms (Figure S2) reveal that the adsorbed amount of template molecules increased rapidly with the increase of concentration of acephate until the adsorption equilibrium was obtained. Furthermore, the amount of acephate adsorbed by MIP was more than that by NIP, indicating that MIP had larger binding capacity than NIP.

The binding affinity and theoretical binding site for acephate of the MIP were evaluated by Scatchard analysis.⁵³ The Scatchard equation is expressed as follows:

$$\frac{Q_e}{C_e} = \frac{Q_m - Q_e}{K_D} \quad (10)$$

where Q_e is the equilibrium binding capacity ($\mu\text{g/g}$), Q_m ($\mu\text{g/g}$) is the maximum binding capacity, K_D ($\mu\text{g/mL}$) is the dissociation constant of the binding sites, and C_e represents the equilibrium concentration of acephate.

The Scatchard plot for MIP [Figure 7(A)] could be separated into two lines with different slopes, indicating that there were two classes of binding sites (nonspecific binding sites and specific binding sites) in MIP, and the rebinding sites were mainly dependent on hydrogen bonding. The linear regression equations for the two linear regions were fitted to be $Q_e/C_e = -4.1828Q_e + 89.503$ ($R^2 = 0.9961$) and $Q_e/C_e = -0.6137Q_e + 22.802$ ($R^2 = 0.9707$). The calculated K_D values were $0.2391 \mu\text{g/mL}$ and $1.629 \mu\text{g/mL}$, and the Q_m values were $3.93 \times 10^3 \mu\text{g/g}$ and $6.81 \times 10^3 \mu\text{g/g}$, respectively. For NIP [Figure 7(B)], only one kind of binding site for acephate can be observed. The fitted linear equation was $Q_e/C_e = -0.2704Q_e + 5.1004$, and the Q_m ($3.46 \times 10^3 \mu\text{g/g}$) and K_D ($3.698 \mu\text{g/mL}$) were calculated. All of the Scatchard results indicate

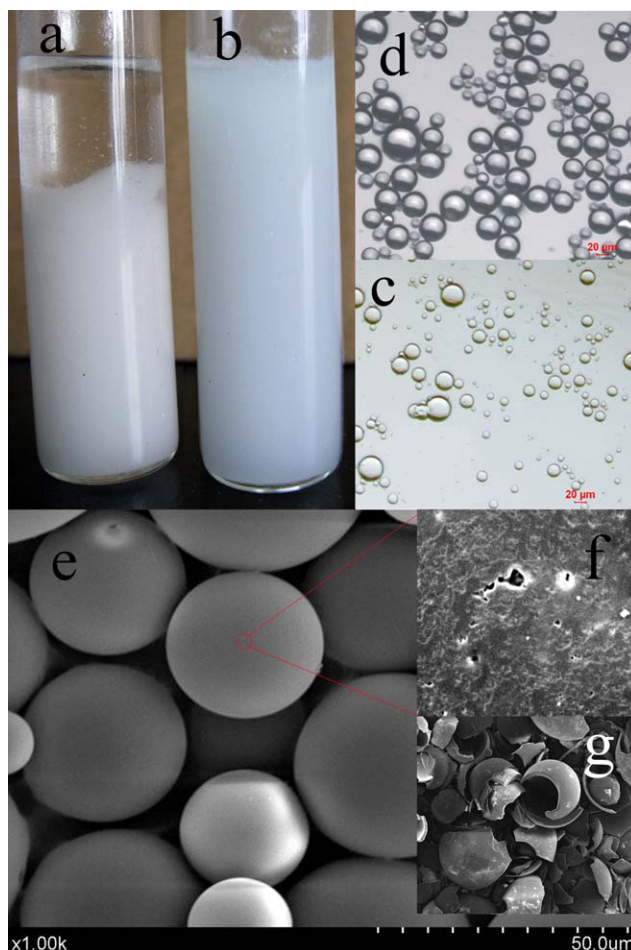


Figure 4. Photographs of the Pickering emulsion before (a) and after (b) ultrasonication; optical micrographs of Pickering emulsions before (c) and after (d) polymerization; SEM micrographs (e) of prepared MIP particles with the surface morphology (f) and hollow core (g). [Color figure can be viewed in the online issue, which is available at wileyonlinelibrary.com.]

that the affinity and binding capacity of MIP were significantly larger than that of NIP.

Selectivity Analysis. Generally, the sites formed in MIP created by the template molecules can lead to much greater selectivity for the imprinted molecule, in comparison with NIP. In order

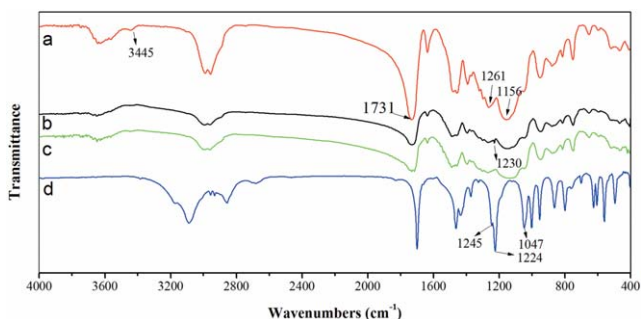


Figure 5. FTIR spectra of NIP (a), MIP without (b) and after (c) extraction of template molecule, and acephate (d). [Color figure can be viewed in the online issue, which is available at wileyonlinelibrary.com.]

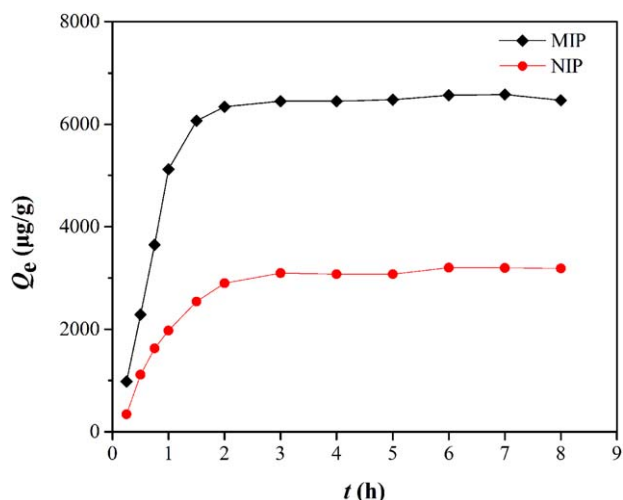


Figure 6. Kinetic binding curves of MIP or NIP particles (20 mg) toward 100 $\mu\text{g/mL}$ acephate in ultrapure water (5 mL) at room temperature. [Color figure can be viewed in the online issue, which is available at wileyonlinelibrary.com.]

to estimate the selectivity of MIP to acephate, structural analogs, such as methamidophos, isocarbophos, and malathion, were used as potential interferents for the selective recognition study. Figure 8 shows that MIP exhibits better binding capacity to the template than to analogs, indicating that MIP provides high adsorption selectivity toward template molecules. It still can be obviously seen that NIP has a certain adsorption of acephate and analogs, but the difference was inconspicuous. On the other hand, the binding capacity of MIP toward methamidophos was higher than other analogs, which can be explained by the fact that the chemical construction and size of methamidophos are more similar to acephate than that of other analogs.

In several selectivity experiments, the binding capacity can be explained by parameters such as the distribution coefficient (K_d), selectivity coefficient (k), and relative selectivity coefficient (k'). They could be calculated according to the equation⁵⁴

Table VI. Adsorption Isotherm Parameters of MIP and NIP Particles toward Acephate

Isotherm models	Parameters	MIP	NIP
Langmuir equation	Q_m ($\mu\text{g/g}$)	6.59×10^3	3.32×10^3
	K ($\text{mL}/\mu\text{g}$)	0.946	0.349
	R^2	0.9998	0.9995
Freundlich equation	K_f ($\mu\text{g/g}$)	3.72×10^3	1.16×10^3
	n^{-1}	0.152	0.273
	R^2	0.7956	0.8186

$$K_d = \frac{Q_e}{C_e} \quad (11)$$

where K_d , Q_e ($\mu\text{g/g}$), and C_e ($\mu\text{g/mL}$) are the distribution coefficient, equilibrium adsorption amount, and the equilibrium concentration of acephate and analogs:

$$k = \frac{K_{d(\text{acephate})}}{K_{d(\text{analogues})}} \quad (12)$$

where k , $K_{d(\text{acephate})}$, $K_{d(\text{analogues})}$ are the selectivity coefficient and distribution coefficient of acephate and analogs, respectively, and

$$k' = \frac{k_{\text{MIP}}}{k_{\text{NIP}}} \quad (13)$$

where k , k_{MIP} , and k_{NIP} are the relative selectivity coefficient and the selectivity coefficient of MIP and NIP, respectively.

The recognition property of MIP was assessed by the imprinting factor (IF), which is defined as

$$IF = \frac{Q_{\text{MIP}}}{Q_{\text{NIP}}} \quad (14)$$

where Q_{MIP} and Q_{NIP} are the binding capacity of the acephate or the analog on MIP and NIP, respectively.

As seen from Table VII, an IF (2.113) was observed, and the K_d and k values of MIP were conspicuously larger than those of NIP, which sufficiently prove that acephate-imprinted sites were

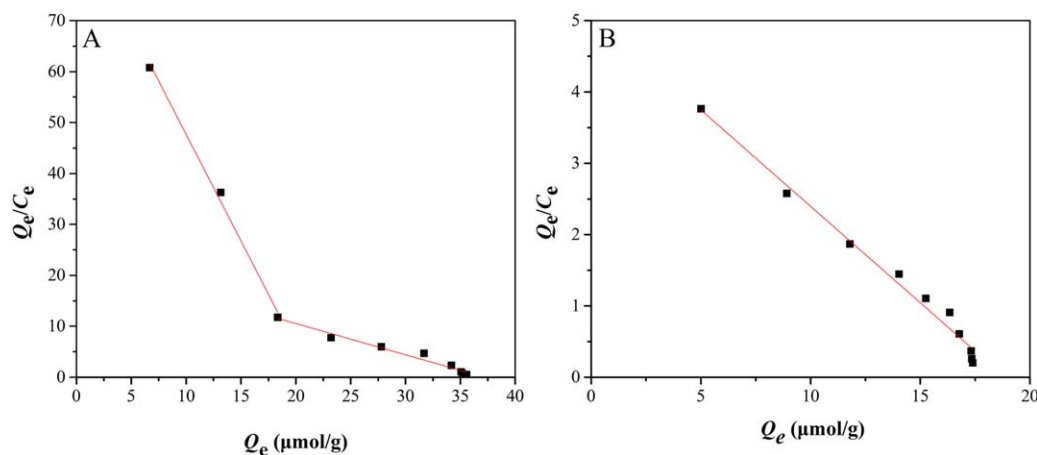


Figure 7. Scatchard plots of the MIP (A) or NIP (B) particles (20 mg) toward acephate with different initial concentrations (5 mL) in ultrapure water at room temperatures. [Color figure can be viewed in the online issue, which is available at wileyonlinelibrary.com.]

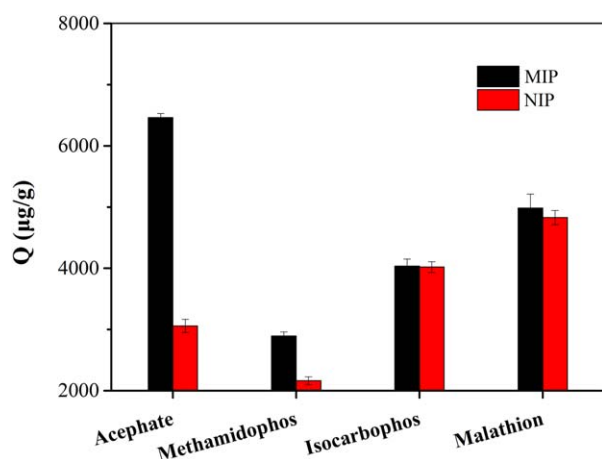


Figure 8. Selective binding of the MIP and NIP toward acephate and analogs. [Color figure can be viewed in the online issue, which is available at wileyonlinelibrary.com.]

formed on MIP during polymerization. The k values of MIP for methamidophos (1.900), isocarbophos (3.128), and malathion (2.864) were calculated, demonstrating that MIP has a higher selectivity for acephate than analogs, which was primarily due to the adsorption specific imprinted sites that are specifically aimed at template molecule. For NIP, the obtained K_d and k values of acephate and analogs were similar, so the adsorption of NIP was nonspecific. The k values for methamidophos (1.723), isocarbophos (2.537), and malathion (2.458) can be calculated, revealing that the MIP had more significant selectivity than the NIP. These results obviously show that the MIP clearly has a high recognition and rebinding affinity for acephate.

Reusability of MIP

To make the MIP economical in practical applications, the reuse of MIP is a critical factor for absorption–desorption performance. Thus, the reusability of MIP was investigated. The absorption–desorption cycle was repeated eight times by using the same MIP to estimate its reusability (Figure S3). It is clearly seen that the binding capacity of MIP is maintained at a high level of over $6.38 \times 10^3 \mu\text{g/g}$ during the eight cycles, which indicates that the imprinted sites were stable enough, and the MIP can be used repeatedly. The average value of eight cycles was calculated to be $6.46 \times 10^3 \mu\text{g/g}$, and the standard deviation (SD) was 0.434.

Table VII. Selective Recognition Parameters of MIP and NIP Particles toward Acephate

Molecules	MIP		NIP			IF
	K_d	k	K_d	k	k	
Acephate	98.306		38.541			2.113
Methamidophos	49.104	1.900	34.943	1.103	1.723	
Isocarbophos	31.423	3.128	31.268	1.233	2.537	
Malathion	34.321	2.864	33.084	1.165	2.458	

Application to Environmental Water

Spiked river, lake, reservoir, and tap water were applied to investigate the application of the MIP in actual water samples. It is obvious (see Figure S4) that the MIP was effective in removing acephate from ultrapure water, river water, and tap water. On the other hand, the removal efficiencies of MIP for acephate in actual water samples are marginally lower than those obtained in ultrapure water, suggesting that the capacity of the MIP to remove acephate in actual water has been reduced. This phenomenon may be explained by the fact that a small quantity of organic or inorganic pollutants in environmental water was adsorbed on the MIP. The binding capacity of MIP, moreover, was still far higher than that of the NIP. The above results reveal the potential of using MIP to remove acephate from environmental water.

CONCLUSIONS

In this work, we combined a computational approach and Pickering emulsion polymerization to prepare an MIP for removing acephate from aqueous solution. A computational method based on DFT was introduced for simultaneous selection of monomer, porogen, and crosslinker. MAA, chloroform, and EGDMA were chosen as the optimal monomer, porogen, and crosslinker, respectively. Then, the water-compatible MIP was prepared via Pickering emulsion polymerization stabilized solely by nano-SiO₂ particles. The results of the characterization tests revealed that a porous and hollow core structure was formed in the MIP. The adsorption performances were also investigated using kinetic, isothermal, selectivity, and Scatchard analyses. The adsorption equilibrium time (3 h), binding amount ($6.59 \times 10^3 \mu\text{g/g}$), and imprinting factor (2.113) of MIP toward acephate were obtained. The high selectivity of the prepared MIP can be attributed to a combined effect of hydrogen bonds and hydrophobic interactions.³⁴ Moreover, the MIP could be reused at least eight times without obvious loss of binding capacity, indicating the potential application of the prepared MIP for selective removal of acephate in aqueous solution.

ACKNOWLEDGMENTS

Financial support was provided by grants from the National Natural Science Foundation of China (30970309, 31201456, and 31371734), Major Scientific and Technological Special Project for “Significant New Drugs Creation” (2009ZX09502~015, 2012ZX09501001), Qing Lan Project, Six Talent Peaks Project of Jiangsu Province, and the project funded by the Priority Academic Program Development of Jiangsu Higher Education Institutions (PAPD).

REFERENCES

1. Aurbek, N.; Thiermann, H.; Szinicz, L.; Eyer, P.; Worek, F. *Toxicol.* **2006**, *224*, 91.
2. Hall, R. J.; Kolbe, E. J. *Toxic. Environ. Health* **1980**, *6*, 853.
3. Chukwudebe, A. C.; Hussain, M. A.; Oloffs, P. C. J. *Environ. Sci. Health, Part B* **1984**, *19*, 501.
4. Li, R.; Liu, Y.; Zhang, J.; Chen, K.; Li, S.; Jiang, J. *Appl. Microbiol. Biotechnol.* **2012**, *94*, 1553.
5. Jain, R.; Garg, V. *Appl. Biochem. Biotechnol.* **2013**, *171*, 1473.
6. Dai, K.; Peng, T.; Chen, H.; Liu, J.; Zan, L. *Environ. Sci. Technol.* **2009**, *43*, 1540.
7. Fadaei, A. M.; Dehghani, M. H. *Res. J. Chem. Environ.* **2012**, *16*, 104.
8. Sarkouhi, M.; Shamsipur, M.; Hassan, J. *Environ. Monit. Assess.* **2012**, *184*, 7383.
9. Cycon, M.; Wojcik, M.; Piotrowska-Seget, Z. *Chemosphere* **2009**, *76*, 494.
10. Zhang, Z. H.; Jiatieli, J.; Liu, D. N.; Yu, F. Y.; Xue, S.; Gao, W.; Li, Y. Y.; Dionysiou, D. D. *Chem. Eng. J.* **2013**, *231*, 84.
11. Al-Qurainy, F.; Abdel-Megeed, A. *World Appl. Sci. J.* **2009**, *6*, 987.
12. Bhadbhade, B. J.; Sarnaik, S. S.; Kanekar, P. P. *J. Appl. Microbiol.* **2002**, *93*, 224.
13. Zhang, Y.; Hou, Y.; Chen, F.; Xiao, Z.; Zhang, J.; Hu, X. *Chemosphere* **2011**, *82*, 1109.
14. Yatmaz, H. C.; Uzman, Y. *Int. J. Electrochem. Sci.* **2009**, *4*, 614.
15. Shah, B.; Jadav, P.; Shah, A. *Environ. Prog. Sustain. Energy* **2014**, *33*, 114.
16. Jusoh, A.; Hartini, W. J. H.; Ali, N. A.; Endut, A. *Bioresour. Technol.* **2011**, *102*, 5312.
17. Zhang, Y.; Pagilla, K. *Desalination* **2010**, *263*, 36.
18. Das, S. K.; Khan, M. M. R.; Guha, A. K.; Das, A. R.; Mandal, A. B. *Bioresour. Technol.* **2012**, *124*, 495.
19. Zhu, X.; Cai, J.; Yang, J.; Su, Q.; Gao, Y. *J. Chromatogr. A* **2006**, *1131*, 37.
20. Wulff, G.; Sarhan, A. *Angew. Chem. Int. Ed. Engl.* **1972**, *11*, 341.
21. Farrington, K.; Magner, E.; Regan, F. *Anal. Chim. Acta* **2006**, *566*, 60.
22. Shamsipur, M.; Rajabi, H. R. *Microchim. Acta* **2013**, *180*, 243.
23. Anirudhan, T. S.; Divya, P. L.; Nima, J. *React. Funct. Polym.* **2013**, *73*, 1144.
24. Shen, X.; Zhu, L.; Liu, G.; Tang, H.; Liu, S.; Li, W. *New J. Chem.* **2009**, *33*, 2278.
25. Chianella, I.; Guerreiro, A.; Moczko, E.; Caygill, J. S.; Piletska, E. V.; De Vargas Sansalvador, I. M. P.; Whitcombe, M. J.; Piletsky, S. A. *Anal. Chem.* **2013**, *85*, 8462.
26. Krupadam, R.; Patel, G.; Balasubramanian, R. *Environ. Sci. Pollut. Res.* **2012**, *19*, 1841.
27. Herrero-Hernández, E.; Rodríguez-Gonzalo, E.; Rodríguez-Cruz, M. S.; Carabias-Martínez, R.; Sánchez-Martín, M. J. *Int. J. Environ. Sci. Technol.* **2015**, *12*, 3079.
28. Rajabi, H. R.; Shamsipur, M.; Pourmortazavi, S. M. *Mat. Sci. Eng.* **2013**, *C33*, 3374.
29. Murray, A.; Örmeci, B. *Environ. Sci. Pollut. Res.* **2012**, *19*, 3820.
30. Chen, L.; Xu, S.; Li, J. *Chem. Soc. Rev.* **2011**, *40*, 2922.
31. Shen, X.; Ye, L. *Macromolecules* **2011**, *44*, 5631.
32. Hunter, T. N.; Pugh, R. J.; Franks, G. V.; Jameson, G. J. *Adv. Colloid Interface Sci.* **2008**, *137*, 57.
33. Colver, P. J.; Colard, C. A. L.; Bon, S. A. F. *J. Am. Chem. Soc.* **2008**, *130*, 16850.
34. Shen, X.; Ye, L. *Chem. Commun.* **2011**, *47*, 10359.
35. Nicholls, I.; Andersson, H.; Golker, K.; Henschel, H.; Karlsson, B. G.; Olsson, G.; Rosengren, A.; Shoravi, S.; Suriyanarayanan, S.; Wiklander, J.; Wikman, S. *Anal. Bioanal. Chem.* **2011**, *400*, 1771.
36. Yang, W.; Liu, L.; Zhou, Z.; Qiu, C.; Ma, P.; Liu, H.; Xu, W. *New J. Chem.* **2013**, *37*, 2758.
37. Khan, M. S.; Krupadam, R. J. *Comb. Chem. High Throughput Screening* **2013**, *16*, 682.
38. Zhou, Q.; He, J.; Tang, Y.; Xu, Z.; Li, H.; Kang, C.; Jiang, J. *J. Chromatogr. A* **2012**, *1238*, 60.
39. Muhammad, T.; Nur, Z.; Piletska, E. V.; Yimit, O.; Piletsky, S. A. *Analyst* **2012**, *137*, 2623.
40. Zhu, G.; Fan, J.; Gao, Y.; Gao, X.; Wang, J. *Talanta* **2011**, *84*, 1124.
41. Murphy, J.; Riley, J. P. *Anal. Chim. Acta* **1962**, *27*, 31.
42. Frisch, M.; Trucks, G.; Schlegel, H.; Scuseria, G.; Robb, M.; Cheeseman, J.; Montgomery, Jr., J.; Vreven, T.; Kudin, K.; Burant, J. Gaussian 03; Gaussian Inc.: Pittsburgh, PA, **2003**.
43. Atta, N. F.; Hamed, M. M.; Abdel-Mageed, A. M. *Anal. Chim. Acta* **2010**, *667*, 63.
44. Tarannum, N.; Singh, M. *Amer. J. Anal. Chem.* **2011**, *2*, 909.
45. Khan, M.; Wate, P.; Krupadam, R. J. *Mol. Model.* **2012**, *18*, 1969.
46. Tomasi, J.; Persico, M. *Chem. Rev.* **1994**, *94*, 2027.
47. Shen, X.; Xu, C.; Ye, L. *Soft Matter* **2012**, *8*, 7169.
48. Ferreira, S. L. C.; Souza, A. S.; Brandao, G. C.; Ferreira, H. S.; dos Santos, W. N. L.; Pimentel, M. F.; Vale, M. G. R. *Talanta* **2008**, *74*, 699.
49. Gholivand, M. B.; Karimian, N.; Malekzadeh, G. *Talanta* **2012**, *89*, 513.
50. Zhu, Q.-H.; He, J.-F.; Feng, J.-Y. *Eur. Polym. J.* **2007**, *43*, 4043.
51. Zhang, Z.; Tan, W.; Hu, Y.; Li, G.; Zan, S. *Analyst* **2012**, *137*, 968.
52. Anirudhan, T. S.; Rejeena, S. R.; Tharun, A. R. *Ind. Eng. Chem. Res.* **2013**, *52*, 11016.
53. Wu, Z.; Joo, H.; Lee, K. *Chem. Eng. J.* **2005**, *112*, 227.
54. An, F.; Gao, B.; Feng, X. *J. Hazard. Mater.* **2008**, *157*, 286.